CONTROL STRATEGIES FOR DECENTRALISED CONTROL OF ACTIVE MAGNETIC BEARINGS

Cristiana Delprete, Giancarlo Genta
Dipartimento di Meccanica, Politecnico di Torino, Torino, Italia
Stefano Carabelli
Dipartimento di Automatica e Informatica, Politecnico di Torino, Torino, Italia

ABSTRACT
Decentralised or decoupled control has proved to be effective in the basic task of controlling active magnetic bearings. A natural generalisation of proportional (stiffness) and derivative (damping) control actions is a lead-lag type compensator where the stiffness and the damping may be distributed over the bandwidth. Sharp phase lead profiles may be achieved using complex zeros and poles pairs. Operating in this way it is possible to control the anisotropic behaviour which occurs when a linearization strategy based on a low bias current is applied to a rotor subject to static loading. Different control architectures applied to a five active axes spindle are experimentally tested showing a good behaviour in the supercritical range above the rigid body modes with a smooth critical speeds crossing.

INTRODUCTION
Decentralised or decoupled control, i.e. independent control for each axis, has proved effective in the basic task of controlling active magnetic bearings [1]. More complex and multivariable control structures may be requested by additional specifications on performances as well as to comply to particular design requirements like automatic balancing.
Starting from basic PID controller structures, a natural generalisation of proportional (stiffness) and derivative (damping) control actions is a lead-lag type compensator where the mechanical stiffness and damping are functions of the frequency that can be tailored following the requirements, at least within broad margins.
Relying on the decoupling effect of each feedback loop, different structures of decentralised compensating controllers may be devised depending on specifications for the overall behaviour of the rotating machine (e.g. when the machine has to work over the critical speed corresponding to the first deformation mode).
In the design of stable and minimum phase controllers, the stiffness (gain) and the damping (phase lead) can not be dealt with independently (Bode's theorem). Different phase lead profiles may assure damping on particular frequencies (for example those corresponding to rigid modes or stator resonances) without increasing too much the gain at high frequency and hence exciting supercritical resonances. Sharp phase lead profiles may be achieved using complex zeros and poles pairs in the controller.
The testing of different controllers is made easier by the use of numerical filters based on fast digital processors once quantization (both on signals and on filter coefficients) and aliasing phenomena have been correctly dealt with.
The present paper deals with the above issues both theoretically and experimentally by comparing the performances of different control architectures applied to a five active axes spindle purposely built for performing didactic and research tasks [2].

MOTIVATION
The design of the controllers for safe and reliable operation of magnetically suspended rotors should address the following issues:
- smooth behaviour with low amplitudes in the crossing of the critical speeds corresponding to rigid body modes;
- active control of high frequency modes corresponding to flexible body modes, either for subcritical or supercritical operating condition, as high frequency

modes can be sharply excited by the controller even if the spin speed is low.

The previous issues may be dealt with decentralised controllers in a wide range of practical cases.

For what the rigid modes crossing is concerned a pair of problems are usually encountered:

- anisotropic behaviour of the magnetic bearings due to horizontal spin axis configuration with low bias currents;
- limitation of the orbit amplitude at critical speeds.

The first is essentially a "stiffness problem" that may be dealt with by an anisotropic action on the horizontal and the vertical channels, changing either the loop gain or the bias current. The second is essentially a "damping problem" that has to be dealt with by a careful compromise between the required damping at low frequency and the related amplification at higher frequencies. The limitation of the orbit amplitude at critical speeds may be used as an alternative way to cope with the bearings anisotropy.

For what concerns the active control of high frequency modes it should be stated that the problem of adding an appropriate damping has to be considered both for subcritical and supercritical condition. The unbalance specifications contribute to assess the level of damping action needed.

ANISOTROPY CHARACTERISATION

A magnetically suspended rotor with horizontal spin axis can show the typical behaviour of a rotor on anisotropic supports: elliptical orbits and backward whirling motions. This situation is caused by a load asymmetry, usually due to the self weight, and a symmetry in control loop gains.

In figure 1 is depicted a typical magnetic bearing scheme (see [3], [4]). The overall force exerted on the rotor is

$$F = F_1 - F_2 \tag{1}$$

where

$$F_1 = \begin{cases} K\left(\dfrac{i_1}{t_1}\right)^2 & i_1 \geq 0 \\ 0 & i_1 < 0 \end{cases} \qquad F_2 = \begin{cases} K\left(\dfrac{i_2}{t_2}\right)^2 & i_2 \geq 0 \\ 0 & i_2 < 0 \end{cases} \tag{2}$$

and the constant K takes into account all the constructive bearing parameters. Note that $i' = i'_0 + \Delta i$.

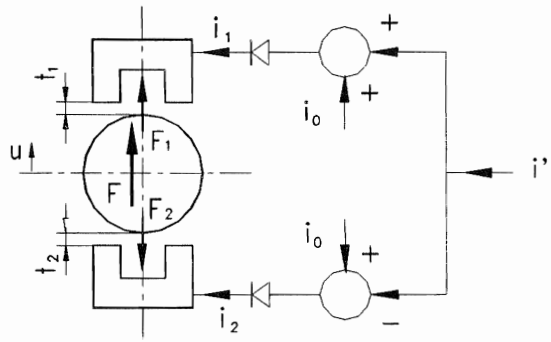

FIGURE 1: Magnetic bearing scheme. The diode symbol means that the current amplifier must go off for negative currents.

The linearized expression of the force around the equilibrium point i'_0 and t'_0 is

$$F_{\text{lin}} = F_0 + k_i \Delta i + k_u \Delta u \tag{3}$$

where

$$\begin{aligned} F_0 &= K\left(\frac{(i_0 + i'_0)^2}{(t_0 - t'_0)^2} - \frac{(i_0 - i'_0)^2}{(t_0 + t'_0)^2}\right) \\ k_i &= 2K\left(\frac{(i_0 + i'_0)}{(t_0 - t'_0)^2} + \frac{(i_0 - i'_0)}{(t_0 + t'_0)^2}\right) \\ k_u &= 2K\left(\frac{(i_0 + i'_0)^2}{(t_0 - t'_0)^3} + \frac{(i_0 - i'_0)^2}{(t_0 + t'_0)^3}\right) \end{aligned} \tag{4}$$

and i_0 is the bias current.

In the nominal gap case ($t'_0 = 0$), the expressions for the unloaded and loaded axis, by computing current i'_0 in order to balance static forces, became respectively

$$\begin{aligned} &F_0 = 0 \quad k_i = 4K\frac{i_0}{t_0^2} \quad k_u = 4K\frac{i_0^2}{t_0^3} \\ &F_0 = W_b \quad k_i = 2K\frac{i_0 + i'_0}{t_0^2} \quad k_u = 2K\frac{(i_0 + i'_0)^2}{t_0^3} \end{aligned} \tag{5}$$

where $i'_0 = t_0\sqrt{W_b/K} - i_0$ and W_b is the rotor weight supported by each bearing.

The resulting mechanical stiffness is

$$k = -k_u + K_c K_A K_T k_i \tag{6}$$

where K_c, K_A and K_T are respectively the stationary gains of the controller, the power amplifier and the position sensor. It should be noted that the mechanical

stiffness depends on the feedback loop gain K_c as well as on the bias current i_0.

CONTROLLER DESIGN

A series of controllers with different architecture has been designed and tested.

The increasing degree of complexity enables the designers to cope with the previously outlined specifications more effectively, the ultimate goal being the active control for supercritical working condition.

Every controller is composed by several sections: a PI stage to guarantee the loop gain and the integral control, and a phase lead multiple stage to guarantee the damping.

As already mentioned, the stiffness problem may be dealt with by the feedback loop gain K_c or the bias current i_0. The PI transfer function common to all the controllers is the following

$$\mathrm{PI}(s) = 3\left(1+\frac{1}{2s}\right) \tag{7}$$

D stage

In series with the PI stage it realises a standard PID controller that has been implemented with a two degrees of freedom structure to overcome the spikes signals generated by the on-line reference position settings.

The basic limitation of this controller is the availability of a single control parameter to cope with the damping action at all the critical speeds.

To assure an adequate damping of the deformation modes, the rigid ones turn out to be only marginally damped (fig.2).; this is usually accepted relying on the self-centred operating condition above them.

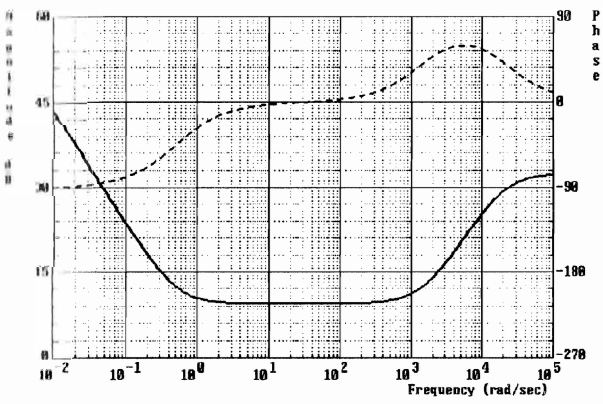

FIGURE 2: Bode's diagrams of the PID controller.

The transfer function of the PID here used is the following

$$\mathrm{PID}(s) = 3\left(1+\frac{1}{2s}+\frac{6.3\cdot10^{-4}\,s}{(6.3\cdot10^{-4}/13)s+1}\right) \tag{8}$$

Lead stage

It has been designed to separately cope with rigid and deformation modes with two distinct lead sections (fig.3). The lead transfer function is

$$C_1(s) = 75\,\frac{s+0.5}{s}\,\frac{s+300}{s+1500}\,\frac{s+3000}{s+15000} \tag{9}$$

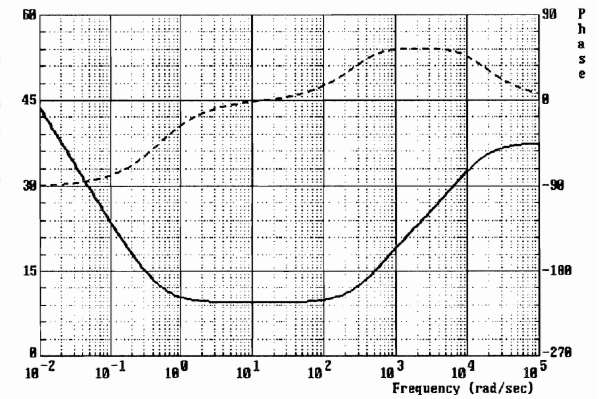

FIGURE 3: Bode's diagrams of the lead controller.

Complex lead stage

In order to achieve a maximum damping action on the first deformation mode with a minimum high frequency gain, a particular lead section has been devised. It relies on the low amplitudes resulting from self-centring in the supercritical range above the rigid body critical speeds, to sharply increase damping up to a pure one (90° phase lead) just before the first flexible body critical speed (fig.4).

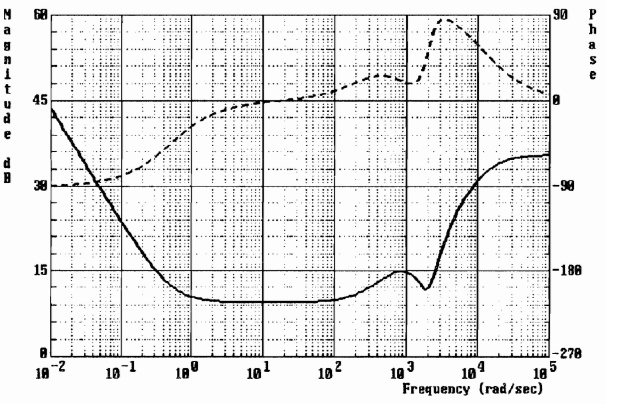

FIGURE 4: Bode's diagrams of the complex lead controller.

The complex lead transfer function is

$$C_2(s) = 60\,\frac{s+0.5}{s}\,\frac{s+300}{s+1500}\,\frac{s^2+1200s+4\cdot10^6}{s^2+13600s+16\cdot10^6} \qquad (10)$$

Figure 5 shows a comparison between the previously described controllers: the use of the antiresonance region between rigid and deformation modes by the complex lead controller should be clear.

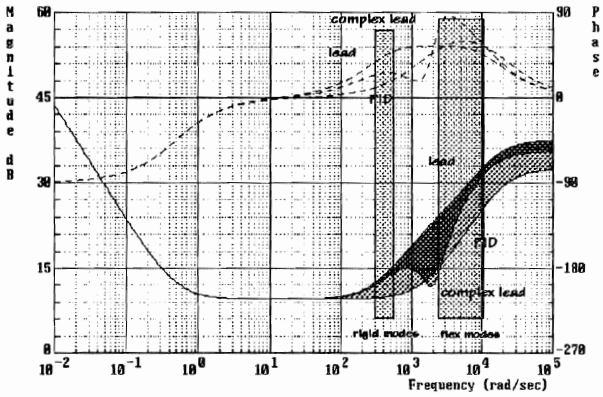

FIGURE 5: Bode's diagrams of the controllers.

EXPERIMENTAL TESTS AND RESULTS

The experimental results reported in the following figures were obtained using the analogic versions of the aforementioned controllers. It should be noted that each controller requires three or five operational amplifier for PID and lead or complex lead respectively. The controllers for the vertical axes are identical to that of the horizontal axes except for the stationary gain that is approximately doubled to take care of the anisotropy introduced by the self weight. The bias current is always taken as one fourth of that required to balance the self weight.

The experimental data are obtained on-line through an HP-IB link to the DVF3 (Digital Vector Filter by Bently-Nevada Co.); Matlab graphical capabilities are then exploited to graphically represent the experimental results.

A new way of representing the orbits of anisotropic systems is here proposed: a tri-dimensional plot in which the orbits are stacked in the third dimension at various speeds. This representation can be labelled as an "orbital tube". The tube shrinks to a point at vanishing speed and, after going through the large amplitude associated with the critical speeds, tends to a circular cylinder with radius equal to the eccentricity in self-centred conditions. The projection on the xy plane, here labelled as "orbital view", gives directly the super-imposition of the orbits: the outer shape of the projection gives the space swept by the centre of the rotor during whirling at all speeds. This projection must be always included within a circle with radius equal to the clearance in order to avoid rotor-stator contact. The projections on the ωx and ωy planes give the peak to peak amplitude at the various speeds: the outer shape of the projection is the usual spin-down curve. In this representation the colour is used as an additional information in terms of amplitude: in a projection on a plane, e.g. ωx, a dark zone indicates high amplitude in any direction.

In the case of the PID controller (fig. 6), the typical behaviour of a rotor on anisotropic bearings is found: elliptical whirling and, in the field between the two critical speeds related to xz and yz planes, backward whirling which at a certain speed becomes circular. In the present case the anisotropy is due to the intrinsic behaviour of the actuator with low bias current. A partial compensation of this anisotropic behaviour is obtained by halfing the gains of the vertical channels, but the anisotropy is still evident: it is not possible to further differentiate the gains owing to the intrinsic limitations of the PID controller featuring just one parameter to define damping.

In the case of the lead controller (fig. 7), the anisotropy can be almost completely compensated and the amplitude at the critical speeds is very small.

The results obtained with the complex lead controller (fig. 8) show a slightly worse behaviour at critical speeds; it has been devised as a trade off between the conflicting requirements of low amplitude at the rigid body critical speeds and almost pure damping at the first three deformation critical speeds.

CONCLUSIONS

Various control strategies for the decentralised control of a five active axes magnetic suspension have been described.

The experimental tests highlight the strong anisotropic behaviour of the actuators due to combined facts of a lateral loading and a low bias current. This effect can not be fully compensated by a conventional PID controller while tests run with lead controllers show an almost complete isotropic behaviour.

The simple lead compensator is more effective in maintaining low amplitudes when crossing the rigid body critical speeds.

The complex lead compensator, while allowing larger amplitudes at low speed, is very effective in damping high frequency modes, where it acts almost as a pure damper.

This last solution has been very effective in avoiding high frequency vibrations which occasionally occurred at any speed with the simpler controllers and offers good prospectives to safely cross the first deformation critical speed.

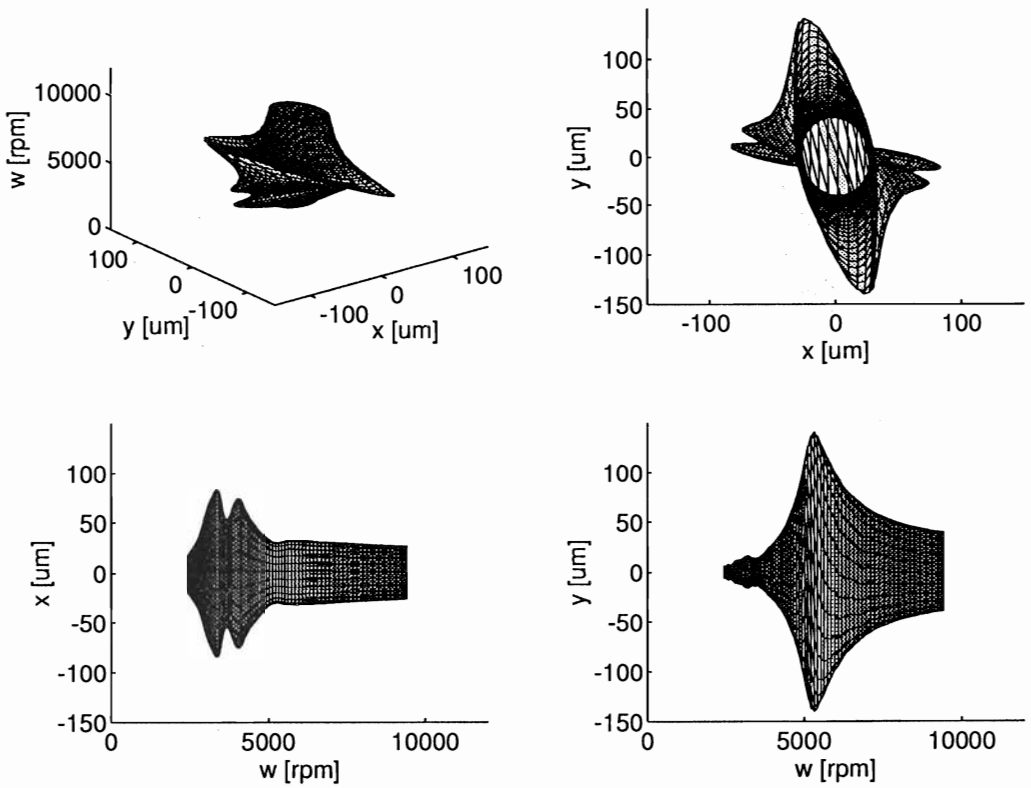

FIGURE 6: PID controller. a) Orbital tube, b) orbital view, c) and d) spin-down curves.

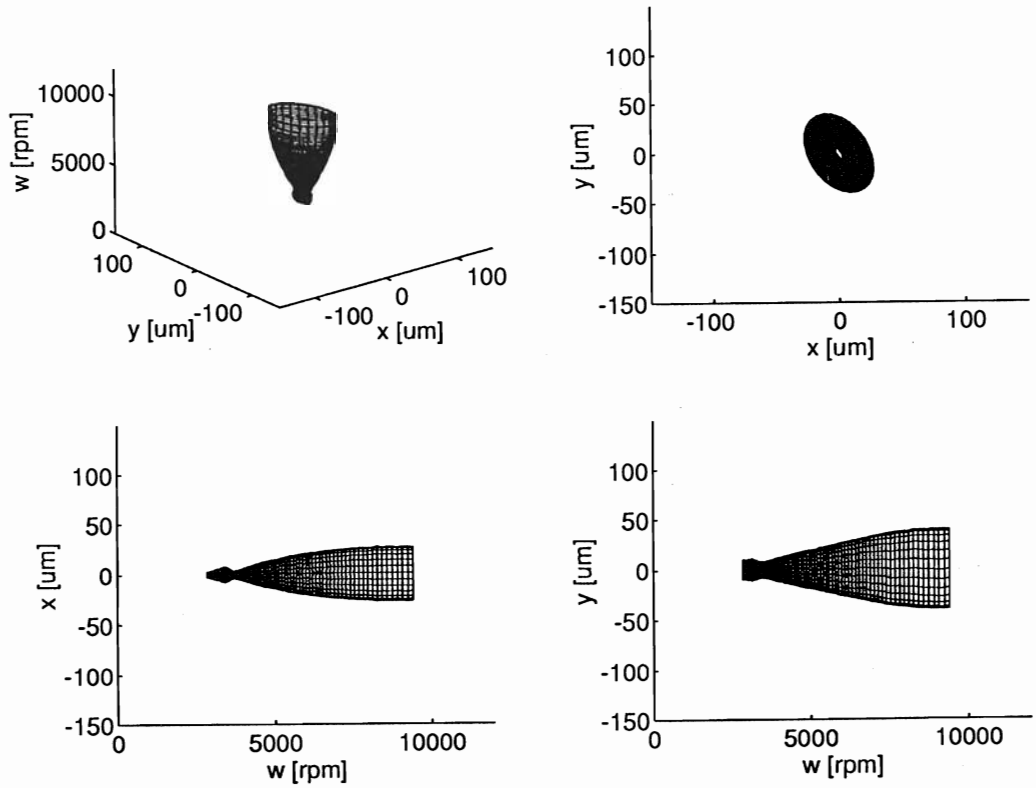

FIGURE 7: Lead controller. a) Orbital tube, b) orbital view, c) and d) spin-down curves.

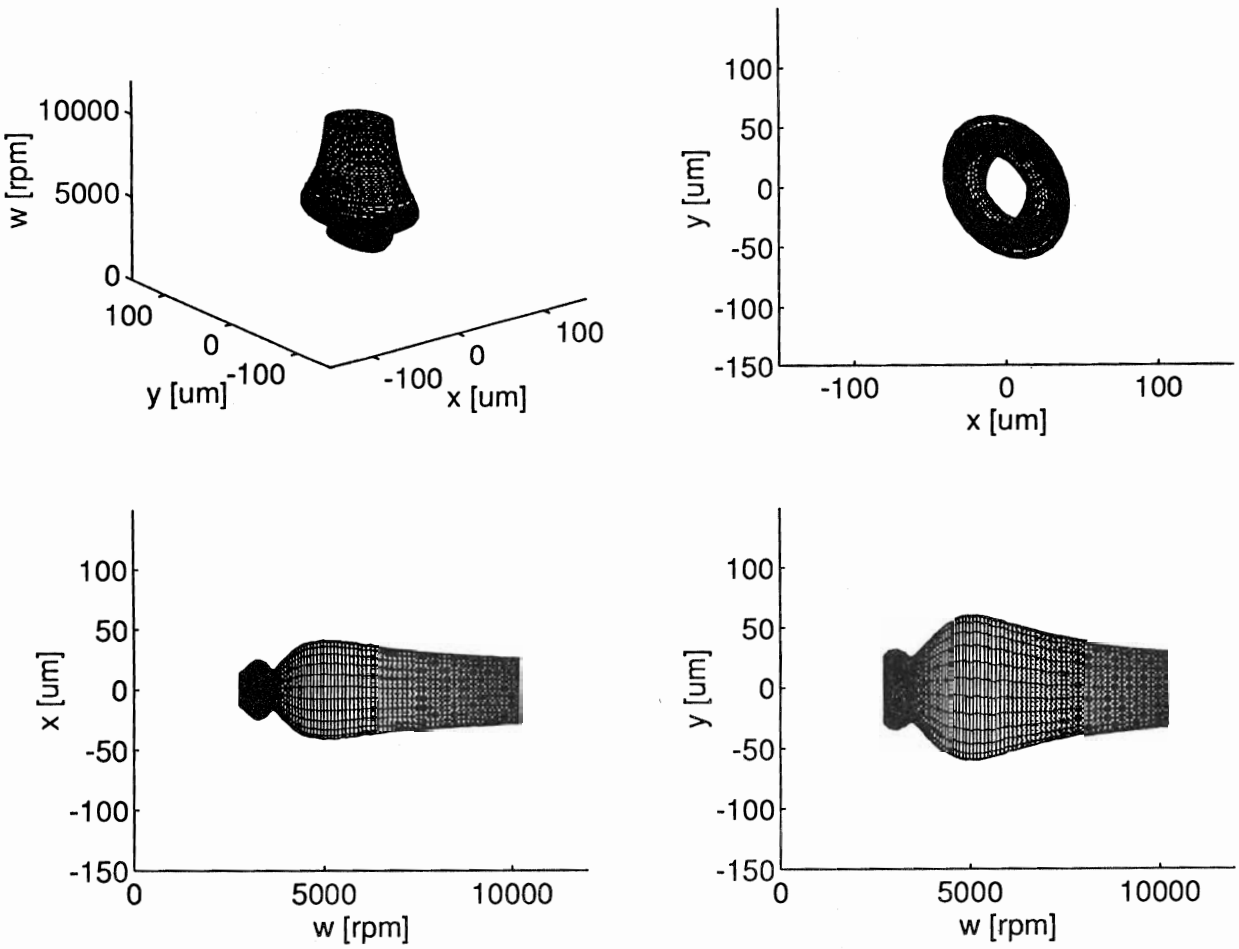

FIGURE 8: Complex lead controller. a) Orbital tube, b) orbital view, c) and d) spin-down curves.

ACKNOWLEDGEMENTS

The present work was partially supported by the National Research Council of Italy under the 93.00539.CT07 grant and by Italian Ministry of University and Scientific Research under the 60% and 40% research grants.

REFERENCES

[1] Larocca P., Fermental D. and Cusson E., Performance Comparison between Centralised and Decentralised Control of the Jeffcott Rotor, Proc. of 2nd Int. Symp. on Magnetic Bearing, Japan, 1990.

[2] Delprete C., Genta G. and S. Carabelli, Design, Construction and Testing of Five-Active Axes Magnetic Bearing System, Proc. of 2nd Int. Symp. on Magnetic Suspension Technology, Washington, 1993.

[3] Schweitzer G., Magnetic Bearings - Applications, Concepts and Theory, JSME Int. Jour., 33, 1990.

[4] Maslen E.H. and Bielk J.R., A Stability Model for Flexible Rotors with Magnetic Bearings, Jour. of Dynamic Systems, Measurements, and Control, 1992.